Sulfuric Acid Dispersion and Injection Engine (SADIE-65)

CONCEPT PROPOSAL

by

Team Skunk-Don't-Works

Gabriel Carey

Xuan Nie

Feb. 16, 2024

Contents

List of Figures

List of Tables

1 INTRODUCTION

1.1 Purpose

The primary objective of the Sulfuric Acid Dispersion and Injection Engine, or SADIE, is to provide an aircraft capable of dispersing aerosol particles into the stratosphere. The aim is to diminish solar radiation absorption by the planet and facilitate artificial cooling of global temperatures. According to the requirements outlined in the RFP, the high-altitude aircraft must have the capability to release these particles at an altitude of 65 000 ft. [1]

1.2 Mission Requirements

Table 1.1: Summary of main RFP requirements.

Specification	Requirement
Cruise Mach	Greater than or equal to 0.5
Capable of flight in icing conditions	Yes, with de-icing device
Certification	Certified to 14 CFR Part 25
Payload capacity	At least 30 000 lb
Cruise range	400 nm
Ferry range	At least 3000 nm
Time-to-climb	Less than or equal to 1 hr
Cruise altitude	65 000 ft
VFR and IFR	Capable of both VFR and IFR flight
Maximum Takeoff and Landing Length	Max T-O length of 8000 ft over a 50 ft obstacle

Key Mission

The key mission requirements from the RFP are summarized in Table 1.1. Most notable are the payload and cruise altitude requirements. A fairly large payload carrying capacity is required, in combination with high altitude flight. As a result, the selected configuration will require a wing design capable of generating ample lift at high altitude, enough to support the moderately heavy weight of the payload along with the inevitably heavy airframe that will result from structural requirements.

1.3 Existing Aircraft

Table 1.2 lists several existing aircraft with similar specifications to the mission requirements listed in Table 1.1. Due to the combination of high-altitude flight and a heavy payload, there is currently a lack of existing aircraft that is capable of handling both of these requirements. Many aircraft can fly at high altitudes, many aircraft can carry large payloads, however few are capable of doing both. Historically, aircraft that have been developed and do meet these stringent requirements tend to fly at supersonic speeds with high operating and production costs, which have not been optimized for the selected mission.

The Boeing B-52 Stratofortress, for example, has great range and payload capacity well exceeding the requirements for the mission, however, the B-52 falls short with a cruise altitude of 50 000 ft. The SR-71 Blackbird was designed as a supersonic reconnaissance aircraft and is capable of flight at an altitude of up to 85 000 ft and can cover a range of over 2000 nm. However, the aircraft only has a payload capacity of 20 000 lb, and flies at speeds far greater than what is necessary for the mission, only lending itself to increased operational and production costs and a more complex design. Similar to the SR-71, the XB-70 meets the cruise range and altitude requirements, however the high supersonic speeds and low payload capacity render it ineffective in completing such a mission.

Table 1.2: Existing aircraft with similar mission capabilities.

Name	Spec	Value	Comparison to desired mission specs
B-52 Stratofortress [2]	Gross Weight	195,000 lb	Within the design range; slightly heavy
	Cruise Speed	510 mph (M 0.772)	Meets the requirement
	Cruise Altitude	50,000 ft	Slightly less than requirement
	Range	6,380 nm 8,685 nm (F)	Far exceeds the requirement of the mission
	Cost	$101 million (Estimated)	The cost is relatively high for the mission
	Payload	70,000 lb	More than double of the requirement
	Thrust	136,000 lb	Slightly more thrust than required
	Gross Weight	60,000 lb	Low; good for design, may increase cost
	Cruise Speed	2,275 mph (M 3.35)	Far too high for the mission; results in increased costs
	Cruise Altitude	80,000 ft	Exceeds the design requirement of 65 000 ft

SR-71 Blackbird [3]	**Range**	2,590 nm (F)	Slightly less than the requirement
	Cost	$322 million	Too high for this mission
	Payload	20,000 lb	Does not meet the requirement
	Thrust	65,000 lb	TWR greater than 1
XB-70 Valkyrie [4]	**Gross Weight**	300,000 lb	Too heavy; too much thrust required
	Cruise Speed	2,056 mph (M 3.11)	Far too high for the mission; results in dramatic increase of costs
	Cruise Altitude	73,000 ft	Exceeds design requirements
	Range	6,600 nm	Far greater than requirement
	Cost	$700 million (Estimated)	Far too high for the mission
	Payload	20,000 lb	Does not meet the requirement
	Thrust	180,000 lb	Too much thrust than what is required

2 CONCEPT SELECTION

2.1 QFD Analysis

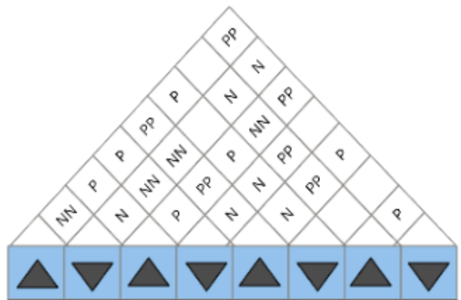

Customer Requirements	Importance 1-5		SIZE OF AIRCRAFT	DRAG	LIFT CAPABILITY	PRODUCTION COST	POWER	WEIGHT	ALTITUDE	OPERATING COST	OUR DESIGN	COMP 1	COMP 2
FAST	2	9.09	3	9	3	9	9	9	3	9	2	4	1
EFFICENT	4.5	20.45	3	9	9	9	3	3	1	9	4	2.5	4
RELIABLE	4	18.18	1			1	3			3	3.5	2	3.5
PAYLOAD	5	22.73	9	1	9	9	9	9	3	9	2.5	2	3.5
INEXPENSIVE	5	22.73	3	3	3	9	9	9	1	9	3.5	1.5	4
CRUISE ALTITUDE	4.5	20.45	1		9	3	9	9	9	3	4	4	2.5
RANGE	3.5	15.91	1	9	9	3	3	9	3	9	2.5	2.5	4
SUM	22	100.00	4.16	5.00	8.11	8.02	8.39	8.80	3.70	9.34		55.52	
			7.49	9.01	14.61	14.45	15.10	15.84	6.67	16.82			

Figure 2.1: House of Quality for SADIE-65.

In terms of customer criteria, the desired qualities for the aircraft include speed, efficiency, reliability, payload capacity, cost-effectiveness, cruise altitude, and range. Based on certain assumptions and requirements from the RFP, most customers prioritize efficiency, cost, cruise altitude, and payload as the crucial aspects for the design of the aircraft, with speed being of marginal importance.

The engineering challenges involved in this project include typical challenges in aircraft design, such as size, drag, lift capability, production costs, power, weight, altitude, and operating costs. The QFD matrix analysis in Figure 2.1 indicates that solving challenges related to lift capability, power, weight, production and operating costs are of the most importance. From this standpoint, design efforts should be focused on optimizing lift capability and power while minimizing both the weight and cost in the development of the aircraft.

2.2 General Configuration

Configuration #1 – Low Wing w/ Aft-Mounted Engine

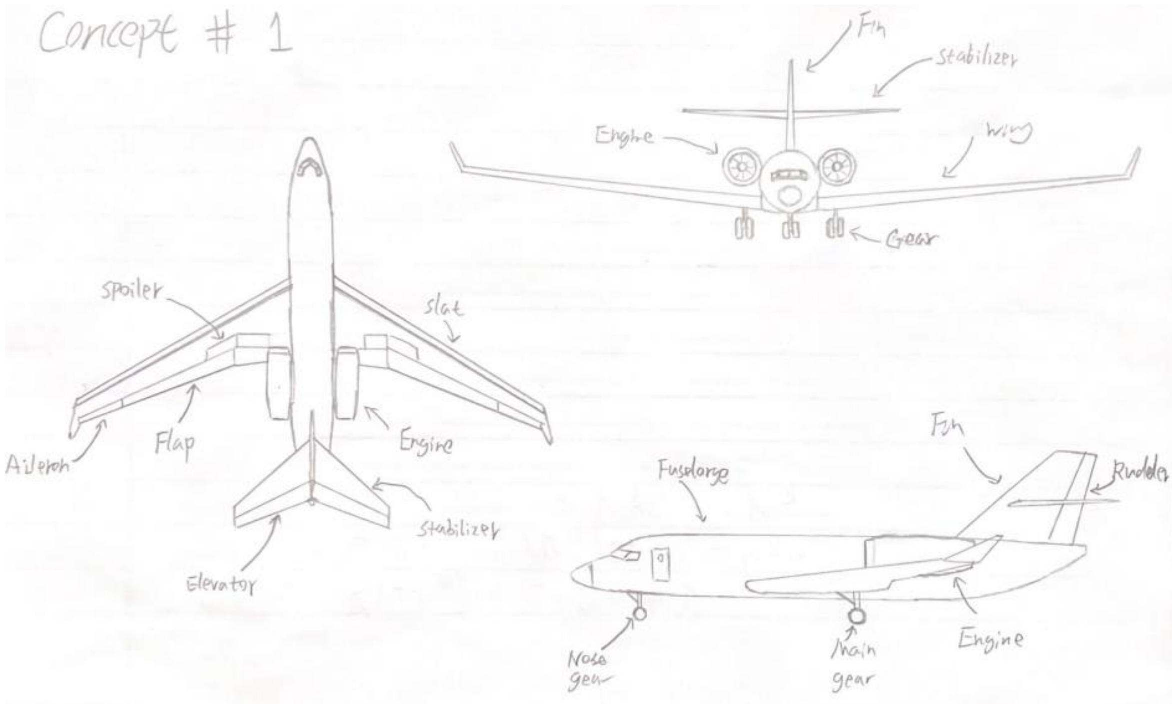

Figure 2.2: Concept sketch of configuration #1.

Configuration #2 – Low Wing w/ Wing-Mounted Engine

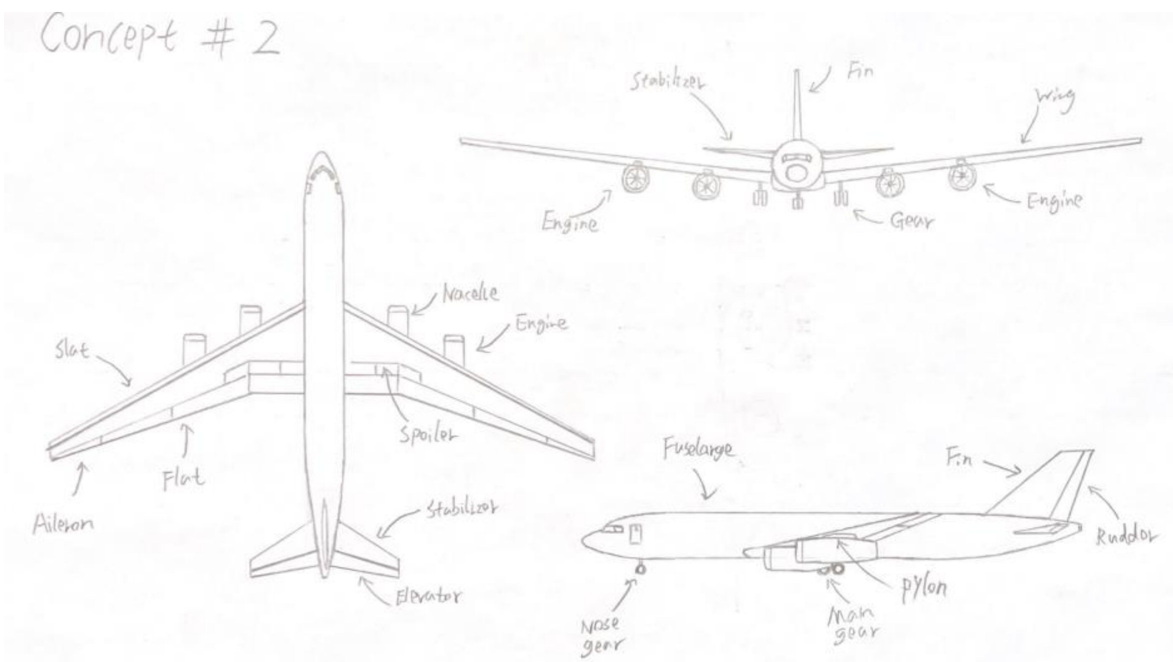

Figure 2.3: Concept sketch of configuration #2.

Concept # 3 – Shoulder Wing w/ Wing-Mounted Engine

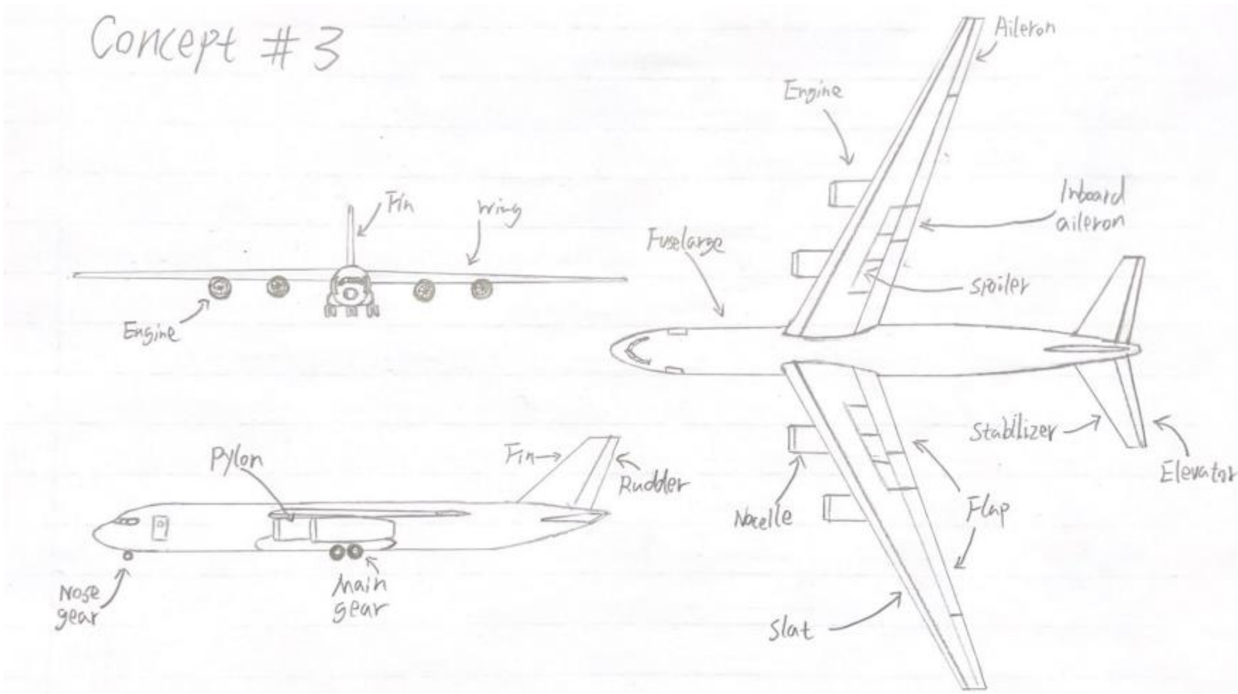

Figure 2.4: Concept sketch of configuration #3 (selected configuration)

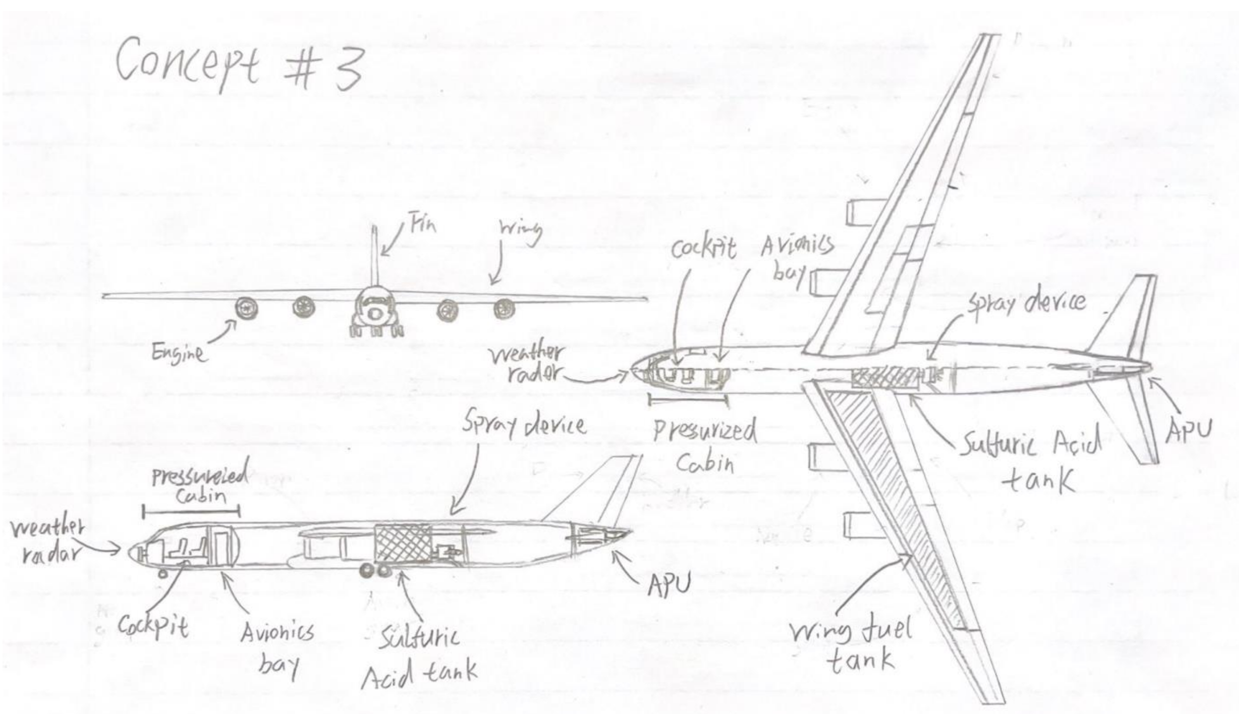

Figure 2.5: Internal concept sketch of selected configuration.

2.2.1 Concept Selection

Among the options considered, the third configuration (Figure 2.4) emerged as the preferred choice over the first two concepts. Due to the dual aft-mounted engine design, the first configuration encounters challenges with weight distribution, exacerbated by the placement of the heavy payload in a relatively short fuselage, forcing the payload tank to be located uncomfortably close to the cockpit. The second configuration features a low-wing design and closely resembles a commercial airliner. However, this concept faced limitations in engine size and upgrade capability due to the minimal clearance between the wing and the ground. This problem was solved in the final configuration, where the wings were moved to the top of the fuselage to increase the wing-to-ground clearance.

2.2.2 General Configuration of Selected Concept

The SADIE-65 dimensions are approximately 33 meters in length, 7.5 meters in height, with a wingspan of 40 meters. Powering this aircraft are four Pratt & Whitney JT8D-219 engines. The fuel tank is positioned in the main wing and center of the fuselage, while the payload tank is situated in the fuselage behind the main wing. This placement enhances the spray range and minimizes the risk of surface corrosion along the bottom of the fuselage.

2.2.3 Wing Configuration

The shoulder-wing design provides ample space for engine upgrades or replacements, such as accommodating larger diameter engines for future enhancements. With a main wing sweep angle of approximately 30 degrees, the aerodynamic center (center of lift) consistently remains behind the center of gravity, ensuring positive or neutral stability. This ensures that either with or without payload it will still remain within the CG envelope. This design feature contributes to stable flight at high altitudes and better high-speed performance due to an increase in the critical Mach number. The high aspect ratio provides better performance during high altitude flight, making the aircraft easier to control while reducing the cruise speed by generating more lift at higher altitudes due to improved aerodynamic efficiency.

2.2.4 Landing Gear

This design reduces the landing gear height, decreasing dead weight on the landing gear system and enhancing reliability through a simpler design. The retractable gear also improves aerodynamic performance by decreasing drag.

2.2.5 Powerplant Selection

Opting for the shoulder-wing configuration not only reduces the likelihood of foreign object damage (FOD) during takeoff and landing, but also allows the under-wing engines to maintain the center of gravity (CG) in the middle of the aircraft, thereby enhancing overall stability during the whole flight. The quad JT8D-219 engines with low bypass ratio ensures engine performance during high altitude flight.

2.2.6 Internal Layout

The internal layout of the fuselage is shown in Figure 2.5. Located at the fore of the fuselage is the pressurized cockpit where the entirety of the crew resides, and where all flight operations occur. The avionics bay is located at the rear of the cockpit, and a weather radar is found within the radome on the nose of the aircraft. In the unpressurized section of the fuselage, a single payload tank constructed of high-density polyethylene (HDPE) is located behind the main wing, storing the 30 000 lb of sulfuric acid. During cruise, the liquid sulfuric acid is gravity-fed through a globe valve, where it is then ejected through a nozzle out the bottom of the fuselage into the atmosphere. A globe-valve is fitted to the tank to ensure a constant flow rate as the tank is emptied. The auxiliary power unit (APU) is located at the rear of the fuselage.

3 COST ANALYSIS

3.1 Production Costs

This section presents a preliminary cost analysis to estimate the production costs of the project. Production and direct operating costs were estimated using the Eastlake cost analysis model, an adaptation of DAPCA-IV that has been tailored towards GA aircraft. The model uses cost estimating relationships, or CERs, to estimate costs involved in the production and operation of GA and business jet aircraft [5]. These CERs have been formulated using historical data collected from previous development projects, thus it is important to understand that the figures presented below only provide an approximate range for expected costs.

To meet the annual payload-drop requirement of 3 million metric tons of payload per year, a total of 300 aircraft will be produced over a 10-year period. Once the primary batch of aircraft are produced over the first production period, the ensuing fleet of 300 aircraft must each fly an average of 2206 flight hours per year, an average of two flights per day, in order to meet the payload requirements outlined in the RFP. Direct operating costs are evaluated and presented in Section 3.2.

The first three CERs presented in Table 3.1 show the approximate work hours required for engineering, tooling, and manufacturing labour. Hourly rates presented are based on median pay data collected as of February 7th, 2024. All costs presented in this section are in USD, unless stated otherwise.

Table 3.1: Estimation of workhours for project development.

Type	Hours	Median Pay ($/hr)
Engineering	15 813 724	50 [6]
Tooling	9 333 994	30 [7]
Manufacturing	43 728 482	25 [8]

Using the data from Table 3.1, the remaining CERs can be calculated. Table 3.2 lists the costs which contribute to the fixed cost of the project, and Table 3.3 lists the costs which contribute to the variable costs, as well as the total cost and selling price. The minimum selling price is a combination of the total cost per unit and liability insurance, the latter of which was assumed to be 15% of the total cost per unit. Based on the minimum selling price, the target selling price was selected at $50 million, with a markup of 37.5%.

Table 3.4 lists the prices of all required vendor supplied components, or VSCs, both with and without a quality discount factor applied. In estimating the variable cost per unit, no QDF was assumed. If a QDF were to be applied, the total cost per unit could be reduced by up to 15%, falling under $27 million.

Table 3.2: Estimation of fixed costs in USD.

CER	Total Cost	Cost per Unit
Total cost of engineering	798 593 074	2 661 977
Total cost of development support	263 716 618	879 055
Total cost of flight operations	19 105 137	63 684
Total cost of tooling	282 820 018	942 733
Fixed cost	1 364 234 847	4 547 449

Table 3.3: Estimation of variable costs in USD.

CER	Total Cost	Cost per Unit
Manufacturing labour	1 104 144 161	3 680 481
Quality control	220 276 760	734 256
Materials/equipment	2 612 166 229	8 707 221
Variable cost (per unit)	-	27 081 957
Total cost per unit	-	31 629 407
Liability insurance	-	4 744 411
Minimum selling price	-	36 373 818
Target selling price per unit	-	**50 000 000**

Table 3.4: Costs of vendor supplied components in USD.

Component	Cost (w/o QDF)	Cost (w/ QDF)
Landing gear	0	0
Complete avionics package [5]	2 000 000	1 311 357
Engine(s) [9]	11 960 000	7 841 915

At a selling price of $50 million USD, the project will break even after selling 75 out of 300 units. Selling all 300 units will yield a revenue of $15 million following the completion of the initial 10-year production period, with a return on investment of 38%. A plot for the break-even analysis is presented in Figure 3.1.

Table 3.5: Project cash flow and break-even analysis.

Total revenue	$15.0 billion
Total cost	$10.9 billion
ROI (300 units sold)	38%
Units to break-even	75

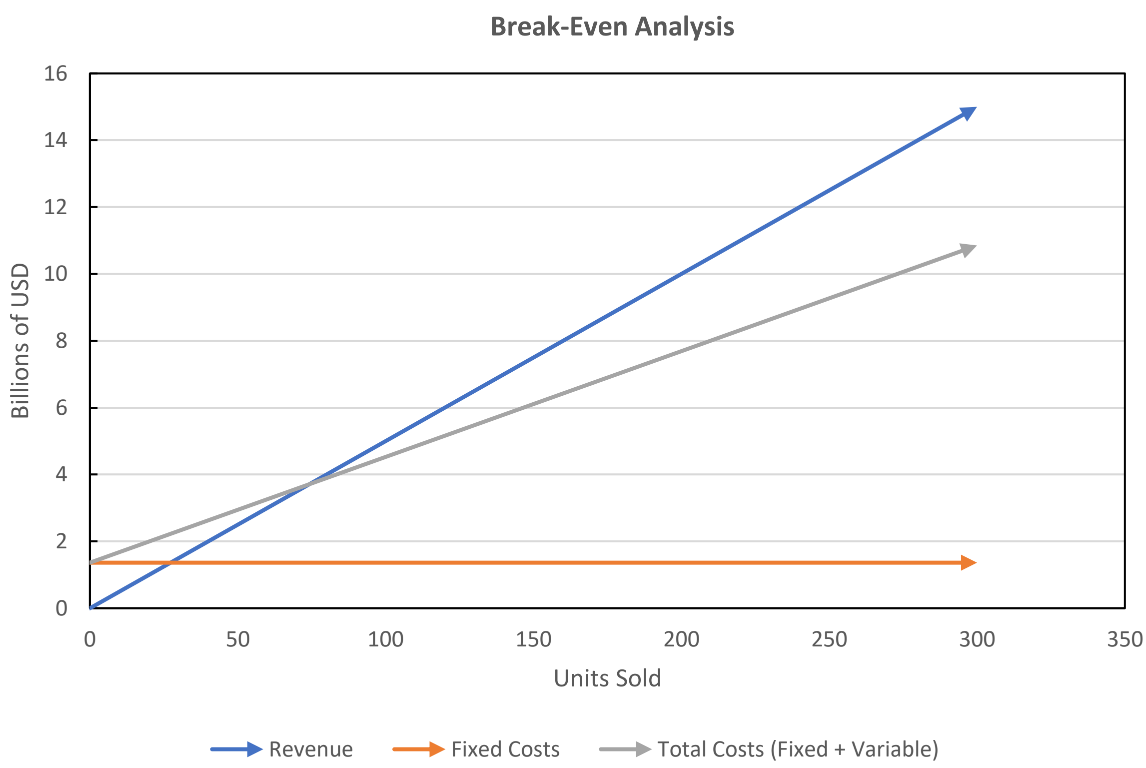

Figure 3.1: Break-even analysis-Comparison of revenue vs total costs and fixed cost.

3.2 Operational Costs

This section estimates the direct operational costs associated with operating a single aircraft. The costs were estimated using simple historical relations for business jet aircraft [5]. Table 3.6 shows the individual operating costs which contribute to the total annual fixed cost. As stated in Section 3.1, each aircraft must complete an average of 2206 flight hours per year in order to meet the desired payload dispersion goal. To compute the maintenance, storage, and fuel costs, the hourly wage of an A&P mechanic was assumed to be $32, which was the median pay for an entry level position as of Feb. 7th, 2024 [10]. The storage cost was assumed to be $3000/month [5], and the price for Jet A1 fuel as of Feb. 15th, 2024, is $2.1/gallon [11]. The crew salary was approximated at $80 an hour [5], with a crew size of four as outlined by the requirements. The engine overhaul fund accounts for all four of the P&W JT8D turbofan engines.

Figure 3.2 shows the distribution of each annual operational cost towards the total annual fixed cost, with the bulk of costs resulting from fuel, due to the high number of yearly flight hours required. Note that any and all aircraft produced and acquired after the initial 10-year production period will join the existing aircraft already in-service, increasing the fleet size, thus reducing the required yearly flight hours per aircraft and the operational costs attributed to each individual aircraft.

Table 3.6: Estimation of direct operational costs in USD.

Cost	Cost ($/year)
Maintenance	225 894
Storage	36 000
Annuel fuel	7 854 831
Annuel insurance	750 500
Annuel inspection	10 000
Engine overhaul	66 180
Crew salary	705 920
Total annual fixed cost	9 649 325

Table 3.7 also shows the operational costs reported in cost per flight hour and cost per nautical mile, as well as the total life-cycle-cost of a single aircraft. The LCC was approximated by using the total annual fixed cost from Table 3.6 and assuming a lifespan of 10 years at a minimum. Each aircraft will cost a total of $146.5 million to acquire and operate for 10 years, with the assumption of a fleet size of 300 and the flight hours required. Acquisition of the entire fleet and operation over the entire 10-year period will cost just under $44 billion. The cost per metric tonne is based on the LCC and the tonnage of payload dispensed over the aircraft's lifecycle.

Table 3.7: Estimation of LCC and variable operational costs.

	Value	Units
Total variable cost per flight hour	4 374	\$/flgthr
Cost per nautical mile	10.85	\$/nm
Cost per metric tonne (of payload)	1 465	\$/Mt
Total life-cycle-cost (LCC)	146 493 251	\$

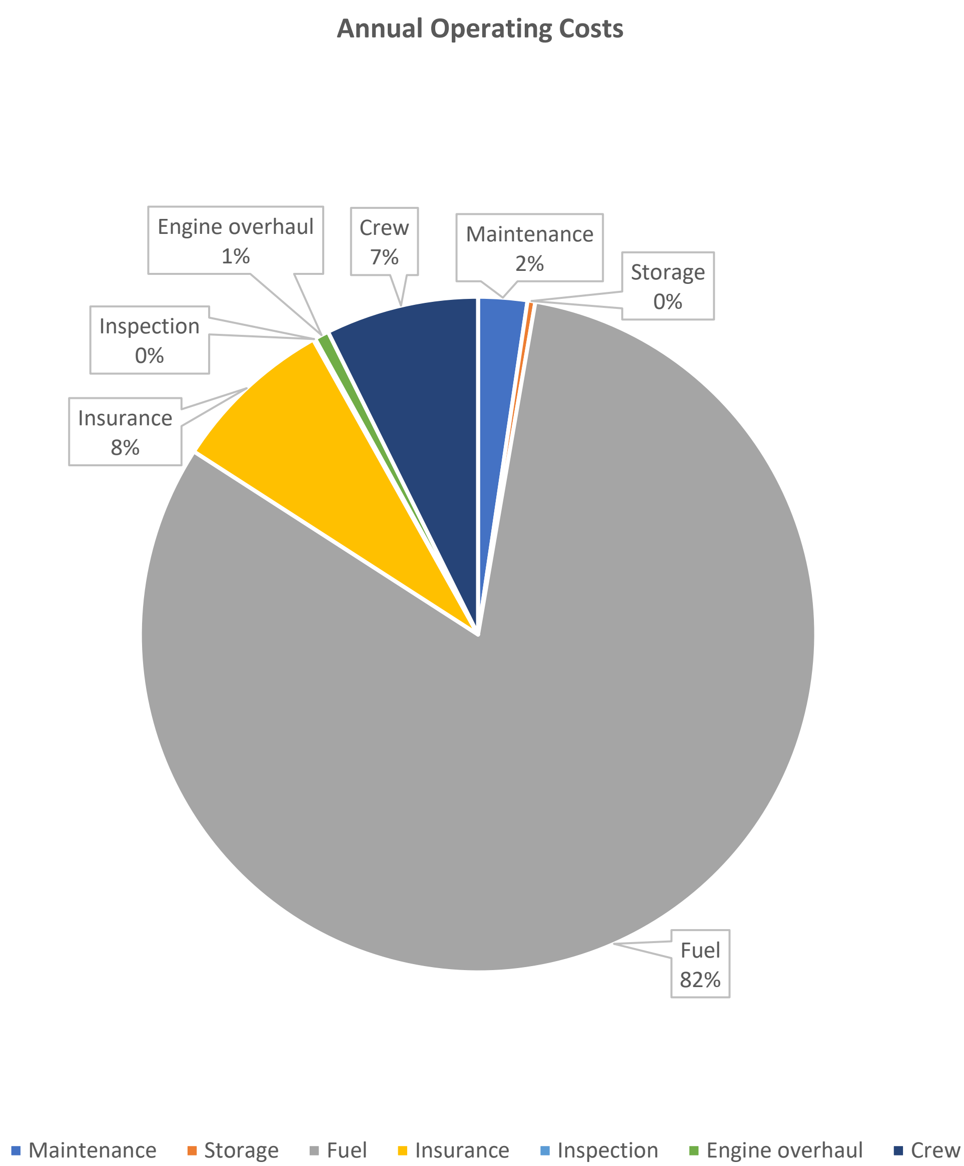

Figure 3.2: Cost distribution of annual DOCs.

4 INITIAL SIZING

4.1 Design Mission Profile

The mission profile for the primary payload-dispensing mission is a simple cruise mission profile, shown in Figure 4.1 [12]. The five main segments consist of: taxi and takeoff, climb, cruise, descend, and landing. Performance parameters optimized for the cruise segment of the mission are listed in Table 4.1. Following takeoff, the aircraft will climb to a cruise altitude of 65 000 feet in 60 minutes. Once at altitude, the cruise segment begins. At this point, the aircraft will cruise for 400 nautical miles at a true airspeed of 400 knots, or Mach 0.70, at a constant altitude. During this time, the payload will be dispensed at a continuous rate until completion of the cruise leg. Once the payload has been fully dispersed into the atmosphere, the plane will descend over the next 45 minutes, followed by landing. The entire duration of the mission is just under 3 hours.

Table 4.1: Preliminary design parameters for the simple cruise mission.

Parameter	Value	Units
Cruise altitude	65 000	ft
Cruise range	400	nm
Cruise speed	400	KTAS
SFC	0.737	lb_f/lbf.hr
Crew Weight	800	lb_f
Payload Weight	30 000	lb_f
Time-to-climb	60	min
Time-to-descend	45	min
Engine cruise thrust	20 960	lb_f
Aspect ratio	11.7	-
Lift-to-drag ratio	17.5	-

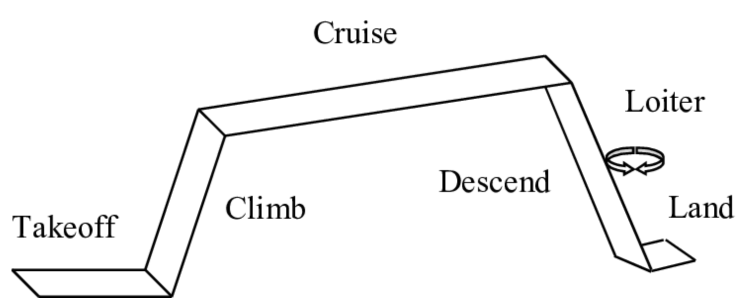

Figure 4.1: The simple cruise mission profile.

4.2 Preliminary Sizing

The sizing analysis that follows provides an estimate for the design gross weight of the aircraft using simple relations for each mission segment in Figure 4.1. The weight analysis process is briefly described below. It is an iterative process, however only the final iteration is presented for simplicity. The methods used can be found in more detail from [13].

To begin the analysis, an arbitrary design gross weight is selected from a range of typical historical values for similar aircraft. These values have been gathered and presented in Table 4.2, along with their respective empty weight fractions. Using the data from this Table, a plot of empty weight fractions vs the logarithm of gross weight was created and is presented in Figure 4.2. By fitting a linear trendline to the data points and matching the predicted gross weight to the trendline, the empty weight fraction can be approximated for the given gross weight. Weight fractions for the final iteration of the weight analysis are shown in Table 4.3. Calculations may be found in Appendix A.

Table 4.2: Historical empty weight fractions of similar aircraft.

Aircraft	W_0 (lb_f)	W_e/W_0
Boeing 727-100 [14]	169 000	0.519
Trident B3 [15]	107 000	0.553
McDonnell Douglas DC-9 [16]	97 000	0.542
Bombardier Global 7500 [17]	114 850	0.537
Gulfstream G650 [18]	99 600	0.542
Gulfstream V [19]	90 500	0.510
Bombardier Global Express [20]	92 500	0.550
Dassault Falcon 7X [21]	70 000	0.523
Boeing 737-600 [22]	144 500	0.555
Airbus A318 [23]	150 000	0.581
Boeing B-47 [24]	133 030	0.601
Boeing B-52 [25]	265 000	0.698
Rockwell B-1 [26]	326 000	0.589

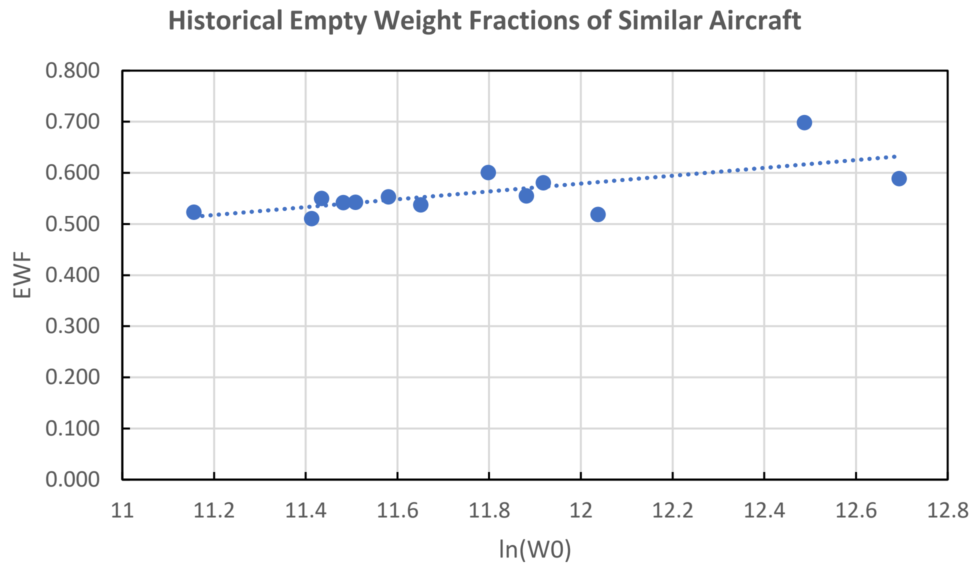

Figure 4.2: Empty weight fraction relations for similar aircraft.

After determining the empty weight fraction, the fuel weight fraction is determined. This value is obtained by first computing the product of each weight fraction for each individual mission segment, which provides the final landing weight of the aircraft, which is equal to the sum of empty and crew weights. The difference between the starting takeoff weight and the final landing weight is the amount of fuel burned to complete the mission, dividing by the gross weight yields the fuel weight fraction. However, due to the unique nature of the payload delivery for this particular mission, the loss of payload must be accounted for when determining the fuel weight. Similarly, when determining the weight fraction for the cruise segment, this gradual payload drop must be accounted for on top of the fuel consumption. This was accomplished by determining the weight fractions for several incremental steps of the cruise leg for every certain number of nautical miles covered. The product of all these weight fractions yielded the final weight fraction for the entire cruise leg.

In determining these weight fractions, several assumptions were made. During taxi & takeoff, the following assumptions were made: (1) The idle thrust-to-weight ratio (TWR) was approximated as 7% of the max thrust, (2) The aircraft taxis for 20 minutes, and (3) Engines operate at max thrust for 1 minute during takeoff. The best lift-to-drag ratio for the best range was approximated as 86.6% of the maximum lift-to-drag. The thrust for the entire mission was assumed to be constant at the cruise thrust, with a constant cruise SFC. A sensitivity study was conducted on the final gross weight by varying several of these parameters, and by analyzing the results, it can be noted that such assumptions do not have a great effect on the final weight. The full sensitivity analysis is presented in Section 4.3. All mission specifications used for the sizing analysis can be found in Table 4.1.

Table 4.3: Sizing analysis weight fractions for final iteration.

Weight Fraction	Value
Taxi & T-O	0.996
Climb	0.899
Cruise (No payload drop)	0.953
Cruise (Payload drop)	0.739
Descend	0.885
Landing	0.990
Total	0.580
Empty Weight	0.574
Fuel Weight	0.224

Table 4.4: Weight upon completion of each mission segment.

Mission Segment	Weight at End of Segment (lb_f)
Taxi & T-O	152 393
Climb	136 946
Cruise	101 156
Descent	89 570
Landing	88 674

With the fuel weight known, the fuel weight fraction can be calculated. Using the empty and fuel weight fractions, along with the payload and crew weights, a new guess for the design gross weight can be calculated. This process is then repeated again with the new calculated design gross weight. This iteration process was repeated until the calculated weights converged. This value is the final design gross weight presented below. Table 4.5 summarizes the final gross weight, along with the remaining significant weight parameters.

Table 4.5: Summary of aircraft weights in lb_f.

Design gross weight	153 011
Empty weight	87 874
Fuel Weight	34 336
Payload weight	30 000
Crew weight	800

Figure 4.3 presents a payload-range study which was conducted with varying payloads and quantities of fuel. The maximum payload for the aircraft is 30 000 lb, with a maximum fuel capacity of 45 000 lb. The study shows the trade-off between payload and fuel, and the effect this has on the cruise range. The leftmost point, point A, carries the maximum amount of payload with no fuel, which thus has a range of zero. To the right is point B, or the design point, which meets the required mission specifications, requiring 34 336 lb of fuel at MTOW. Point C is located down and to the right, which shows the range at maximum fuel capacity and partial payload, still at MTOW. Finally, point D carries maximum fuel with no payload, exhibiting the longest cruise range. A tabulated version of the data points from the plot can be found in Appendix B.

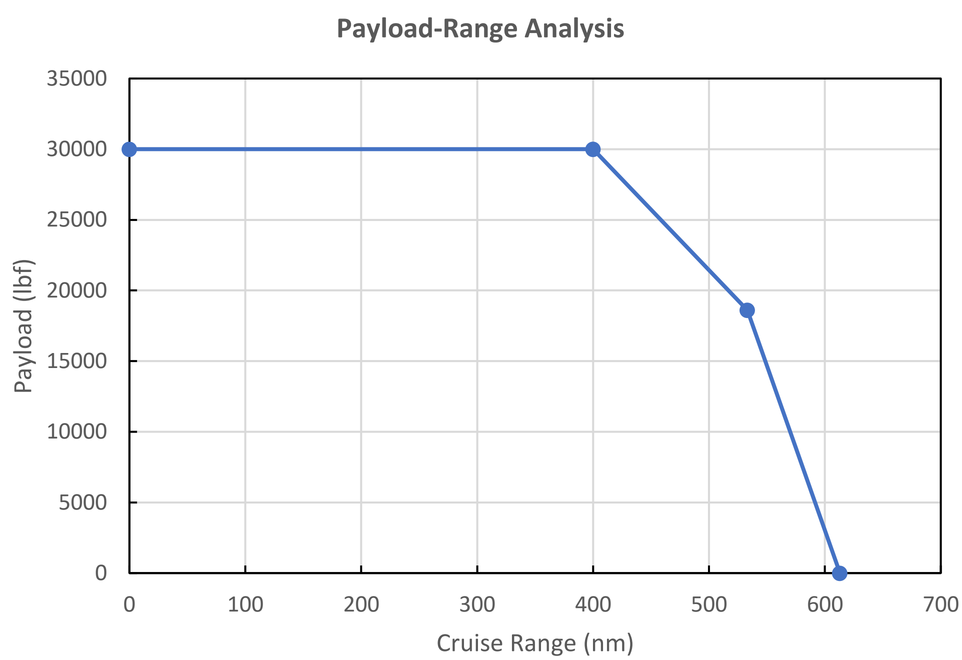

Figure 4.3: Payload-range analysis.

4.3 Sizing Sensitivity

A sensitivity analysis was performed in order to analyze the sensitivity of the design gross weight to several different parameters. The analysis was conducted by calculating the gross weight as a function of only one varying parameter at a time. Each parameter was modified over a fixed range of percentages of its initial value. By a quick inspection of Figure 4.4, it can be easily identified that the gross weight is most sensitive to the empty weight fraction, thus it was crucial that sufficient data was collected in Table 4.2 to generate an accurate relationship between the empty weight fraction and gross weight in order to obtain a valid estimation of the aircraft gross weight.

Second to the EWF, the design gross weight is most sensitive to a decrease in the lift-to-drag ratio. For this reason, the selection of this parameter may be a potential source of error, as it was only approximated using empirical relationships based on historical data. The remaining parameters have a relatively insignificant impact on the final weight, however a lower SFC may result in a slightly lighter aircraft. Different SFCs for different mission segments could potentially influence the gross weight, as the engine SFC was assumed to be constant for the entire duration of the mission. Range and payload data provide little use, as they are fixed values as per the requirements outlined in the RFP. Complete tabulated data used to plot Figure 4.4 can be found in Appendix B.

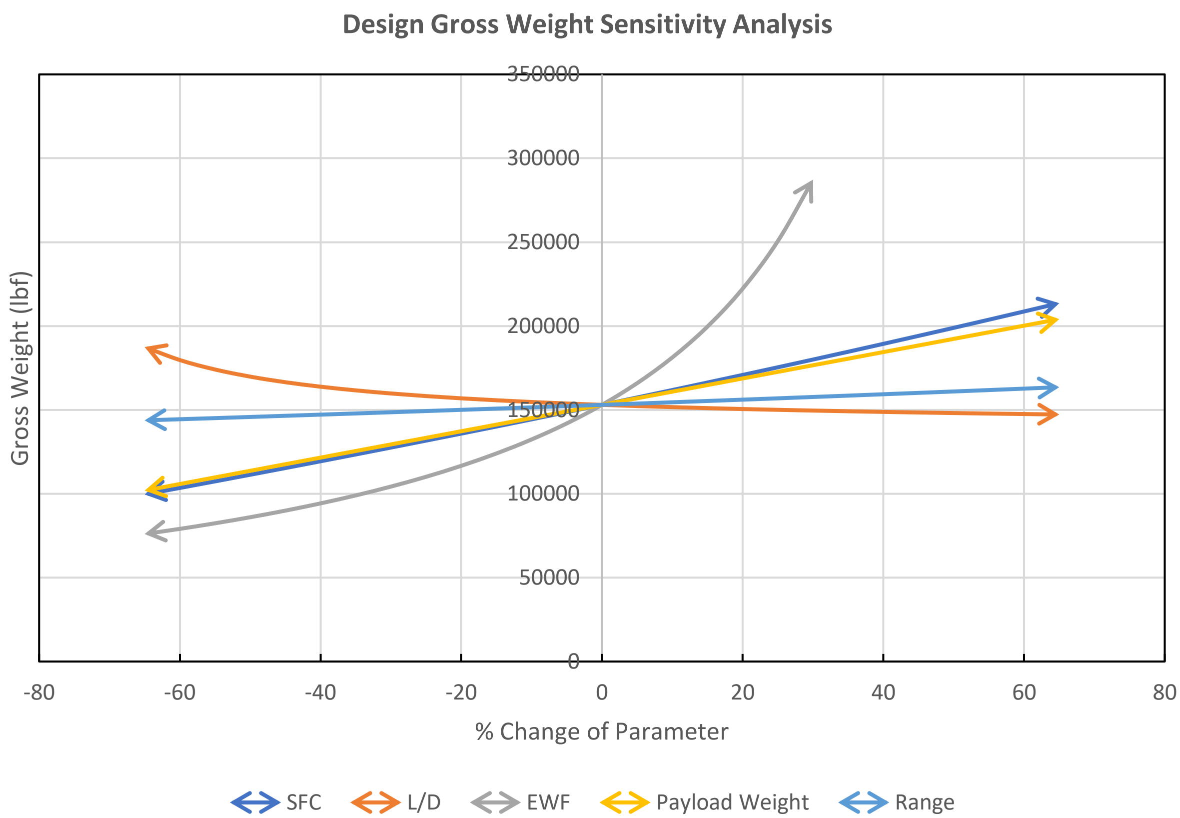

Figure 4.4: Sensitivity analysis on design gross weight.

References

[1] M. Bradley, "Stratospheric Payload Delivery," AIAA, 2023.

[2] Aerospaceweb.org, "Aircraft Museum - B-52 Stratofortress," aerospaceweb.org, [Online]. Available: https://aerospaceweb.org/aircraft/bomber/b52/. [Accessed 15 Feb 2024].

[3] Aerospaceweb.org, "Aircraft Museum - SR-71 Blackbird," Aerospaceweb.org, [Online]. Available: https://aerospaceweb.org/aircraft/recon/sr71/. [Accessed 15 Feb 2024].

[4] Aerospaceweb.org, "Aircraft Museum - XB-70 Valkyrie," Aerospaceweb.org, [Online]. Available: https://aerospaceweb.org/aircraft/research/xb70/. [Accessed 15 Feb 2024].

[5] S. Gudmundsson, "GENERAL AVIATION AIRCRAFT DESIGN," in *Aircraft Cost Analysis*, Elsevier, 2022, pp. 33-54.

[6] "How Much Do Engineer Jobs Pay per Hour?," ZipRecruiter, 8 February 2024. [Online]. Available: https://www.ziprecruiter.com/Salaries/Engineer-Salary-per-Hour. [Accessed 15 February 2024].

[7] "Tooling Specialist Salary," ZipRecruiter, 8 February 2024. [Online]. Available: https://www.ziprecruiter.com/Salaries/Tooling-Specialist-Salary. [Accessed 15 February 2024].

[8] "What Is the Average Manufacturing Salary by State," ZipRecruiter, 2024. [Online]. Available: https://www.ziprecruiter.com/Salaries/What-Is-the-Average-Manufacturing-Salary-by-State. [Accessed 15 February 2024].

[9] L. Jenkinson, P. Simpkin and D. Rhodes, Civil Jet Aircraft Design, Butterworth-Heinemann, 2001.

[10] "Entry Level A&P Mechanic Salary," ZipRecruiter, 8 February 2024. [Online]. Available: https://www.ziprecruiter.com/Salaries/Entry-Level-A-P-Mechanic-Salary. [Accessed 15 February 2024].

[11] "Jet Fuel price Today, 15 February 2024," Jet-A1-Fuel.com, 15 February 2024. [Online]. Available: https://jet-a1-fuel.com/. [Accessed 15 February 2024].

[12] N. V. Nguyen, "The Simple Mission Profile of a Regional Jet Aircraft," 2011.

[13] S. Gudmundsson, "GENERAL AVIATION AIRCRAFT DESIGN," in *Aircraft Weight Analysis*, Elsevier, 2022, pp. 147-155.

[14] "Boeing 727," Wikipedia, 12 February 2024. [Online]. Available: https://en.wikipedia.org/wiki/Boeing_727. [Accessed 15 February 2024].

[15] "Hawker Siddeley Trident," Wikipedia, 2 February 2024. [Online]. Available: https://en.wikipedia.org/wiki/Hawker_Siddeley_Trident#Specifications. [Accessed 15 February 2024].

[16] "McDonnell Douglas DC-9," Wikipedia, 14 February 2024. [Online]. Available: https://en.wikipedia.org/wiki/McDonnell_Douglas_DC-9. [Accessed 15 February 2024].

[17] "Bombardier Global 7500," Wikipedia, 15 February 2024. [Online]. Available: https://en.wikipedia.org/wiki/Bombardier_Global_7500. [Accessed 15 February 2024].

[18] "Gulfstream G650/G700/G800," Wikipedia, 15 February 2024. [Online]. Available: https://en.wikipedia.org/wiki/Gulfstream_G650/G700/G800. [Accessed 15 February 2024].

[19] "Gulfstream V," Wikipedia, 24 December 2023. [Online]. Available: https://en.wikipedia.org/wiki/Gulfstream_V. [Accessed 15 February 2024].

[20] "Bombardier Global Express," Wikipedia, 14 February 2024. [Online]. Available: https://en.wikipedia.org/wiki/Bombardier_Global_Express. [Accessed 15 February 2024].

[21] "Dassault Falcon 7X," Wikipedia, 11 February 2024. [Online]. Available: https://en.wikipedia.org/wiki/Dassault_Falcon_7X. [Accessed 15 February 2024].

[22] "Boeing 737 Next Generation," Wikipedia, 15 February 2024. [Online]. Available: https://en.wikipedia.org/wiki/Boeing_737_Next_Generation#Specifications. [Accessed 15 February 2024].

[23] "Airbus A318," Wikipedia, 14 February 2024. [Online]. Available: https://en.wikipedia.org/wiki/Airbus_A318. [Accessed 15 February 2024].

[24] "Boeing B-47 Stratojet," Wikipedia, 3 February 2024. [Online]. Available: https://en.wikipedia.org/wiki/Boeing_B-47_Stratojet. [Accessed 15 February 2024].

[25] "Boeing B-52 Stratofortress," Wikipedia, 11 February 2024. [Online]. Available: https://en.wikipedia.org/wiki/Boeing_B-52_Stratofortress. [Accessed 15 February 2024].

[26] "Rockwell B-1 Lancer," Wikipedia, 13 February 2024. [Online]. Available: https://en.wikipedia.org/wiki/Rockwell_B-1_Lancer. [Accessed 15 February 2024].

[27] S. Ozgen, *Weight of an airplane and its first estimate,* Middle East Technical University, 2017.

Appendix

A. Sizing Analysis Calculations

The following equations provide sample calculations for the final iteration of the preliminary sizing analysis. Assuming a gross weight of 153 011lbs, the empty weight will first be determined by fitting the logarithm of the gross weight to the trendline in Figure 4.2. The trendline has a slope of 0.0768 and an intercept of -0.3428. The empty weight fraction is calculated as follows:

$$\frac{W_e}{W_0} = A + BlnW_0 = (-0.3428) + (0.0768)\ln(153\ 011) = 0.574$$

Next, the fuel weight fraction is determined. Using the data from Table 4.1, and referencing the nodes from Figure 4.1, the weight fractions for each mission segment can be determined using the following relationships.

$$\frac{W_1}{W_0} = 1 - (\Delta t_{taxi} r_{idle} + \Delta t_{max} r_{max})SFC \qquad \text{(T-O)}$$

$$\frac{W_1}{W_0} = 1 - \big((0.33hr)(0.0096) + (0.017hr)(0.137)\big)(0.737hr^{-1}) = 0.996 \qquad \text{(T-O cont.)}$$

$$\frac{W_2}{W_1} = 1 - \frac{\Delta H * C_t * r_{climb}}{(60)ROC_{avg}} = 1 - \frac{(65000ft)(0.737hr^{-1})(0.138)}{60\left(\frac{1083.3ft}{min}\right)} = 0.899 \qquad \text{(Climb)}$$

$$\frac{W_3}{W_2} = e^{-\frac{R*C_t}{V_{inf}\left(\frac{L}{D}\right)_R}} = e^{-\frac{(400nm)(0.737hr^{-1})}{(400knots)(0.866(17.5))}} = 0.953 \qquad \text{(Cruise-No payload drop)}$$

$$\frac{W_4}{W_3} = 1 - \frac{\Delta H * C_t * r_{descent}}{(60)ROD_{avg}} = 1 - \frac{(65000ft)(0.737hr^{-1})(0.207)}{60\left(\frac{1444.4ft}{min}\right)} = 0.885 \qquad \text{(Descend)}$$

$$\frac{W_5}{W_4} = 0.99 \qquad \text{(Landing)}$$

Taking the product of all of the mission segment weight fractions calculated above, the total mission weight fraction can be determined and used to find the fuel weight fraction.

$$\frac{W_N}{W_0} = \prod_{i=1}^{N}\left(\frac{W_i}{W_{i-1}}\right) = (0.996)(0.899)(0.739)(0.885)(0.99) = 0.580 \qquad \text{(Total)}$$

$$\frac{W_f}{W_0} = 1 - \frac{W_N}{W_0} + \frac{W_p}{W_0} = 1 - 0.580 - \frac{30000}{153011} = 0.224 \quad \text{(FWF)}$$

With the empty and fuel weight fractions known, a new gross weight can be calculated using the following equation.

$$W_0 = \frac{W_c + W_p}{1 - \left(\frac{W_e}{W_0}\right) - \left(\frac{W_f}{W_0}\right)} = \frac{(800) + (30000)}{1 - (0.574) - (0.224)} = 153011$$

These calculations are then repeated using the design gross weight calculated above as the new guess. This process is iterated until the gross weights converge, and the guessed gross weight is equal to the calculated gross weight.

B. Sensitivity Study and Payload-Range Data

Table B.1: Tabulated data for sensitivity analysis plot (Figure 4.4).

	Estimated Design Gross Weight (lb_f)				
% Change	**SFC**	**L/D**	**EWF**	**Payload**	**Range**
-65	99597	187487	76032	101892	143756
-60	103480	179704	79093	105824	144428
-55	107399	174082	82410	109757	145106
-50	111354	169831	86018	113689	145791
-45	115346	166503	89957	117621	146482
-40	119375	163828	94274	121553	147180
-35	123441	161631	99025	125485	147884
-30	127546	159794	104281	129418	148595
-25	131690	158235	110127	133350	149314
-20	135873	156896	116666	137282	150039
-15	140096	155733	124032	141214	150771
-10	144360	154714	132390	145146	151510
-5	148664	153813	141955	149079	152257
0	153011	153011	153011	153011	153011
5	157400	152293	165934	156943	153772
10	161832	151645	181242	160875	154542
15	166308	151059	199660	164808	155319
20	170828	150526	222246	168740	156103
25	175393	150039	250594	172672	156896
30	180004	149592	287230	176604	157697
35	184661	149180	336412	180536	158506
40	189366	148800	0	184469	159323
45	194118	148448	0	188401	160149
50	198919	148121	0	192333	160983
55	203770	147816	0	196265	161826
60	208671	147531	0	200197	162678
65	213623	147265	0	204130	163539

Table B.2: Tabulated data for payload-range plot (Figure 4.3).

	Cruise Range (nm)	**W_P**
Point A	0	30000
Point B	400	30000
Point C	533	18605
Point D	613	0